Progress In Electromagnetics Research C, Vol. 96, 59–71, 2019

Design of Dual-Mode Band-Pass Filter with Novel Perturbation Elements

Yong Cheng[1, *], Chengjun Mei[1], and Lei Zhu[2]

Abstract—A compact square patch band-pass filter is proposed in this paper. The dual-mode filter is designed based on a square patch resonator with a complementary split ring resonator (CSRR) split to be used as a perturbation element. The CSRR split is properly embedded in the square patch resonator to perturb electric current distribution on this patch and thus to simultaneously excite a pair of degenerate modes. Using the proposed CSRR elements, the band-pass filter is designed with miniaturized size, and two transmission zeros in stopbands are achieved to improve the selectivity of the filter. The influence of the CSRR elements on the band-pass filter is analyzed in detail. The proposed dual-mode filter is then fabricated and measured. Good agreement over a wide frequency range is achieved between the simulated and measured results. Moreover, in order to further investigate the characteristic of the dual-mode patch filters with CSRR perturbation, a dual-mode filter with a rectangular ring slot is presented for comparative study.

1. INTRODUCTION

In communication systems, microwave filters play an important role. In recent years, scholars have conducted a lot of research to find higher performance filters to meet the requirements in modern communication development. Due to compact size, easy availability, and other aspects of advantages, planar microstrip filters have been widely used so far. In the early 1970's, Wolff first proposed the concept of microstrip dual-mode filter [1]. Dual-mode filters basically consist of dual-mode resonant structures. Dual-mode resonant structures have a pair of degenerate modes. Through a certain perturbation (e.g., slotted and cutting angle), the original electric field distribution of orthogonal degenerate modes will be distorted so as to split and couple these two degenerate modes. Therefore, there will be two resonant circuits in a single resonator, and the number of resonators for a given degree will be reduced by half [2]. Since a dual-mode structure can be utilized for size reduction, a variety of dual-mode microstrip filters have been designed and reported.

So far, researchers have proposed many filter designs for dual-mode and multi-mode structures. In general, several types of dual-mode micro-strip resonators have been available for filter applications, including rings, loops, circle patches or square patches. In addition, microstrip dual-mode filters can be in general divided into planar or multilayer structures according to implementation forms [3, 4]. Due to these different types and structures of microstrip resonators, a variety of microstrip dual-mode filters have been designed. In 1995, a meander loop dual-mode filter was proposed by Hong and Lancaster [5]. In 1997, Cheng proposed the formulas to design a microstrip dual-mode ring filter with two transmission zeros [6]. In [7], microstrip dual-mode loop filters with different perturbation elements were analyzed and compared. A square patch dual-mode filter possessing crossed slots and spur-lines was designed in [8]. A

Received 17 June 2019, Accepted 26 August 2019, Scheduled 25 September 2019

* Corresponding author: Yong Cheng (chengy@njupt.edu.cn).

[1] College of Electronics and Optical Engineering & College of Microelectronics, Nanjing University of Posts and Telecommunications, Nanjing 210023, China. [2] Department of Electrical and Computer Engineering, Faculty of Science and Technology, University of Macau, Macau, China.

single slotted circular patch resonator for a novel dual-mode dual-band BPF design was proposed in [9]. However, compared with patch resonators, rings and loops resonators have their intrinsic drawbacks of higher conductor loss and lower power-handling capability. Thus, patch resonators with low insertion loss and high power handling capacity become more attractive and are often used to design dual-mode filters. For most of patch resonators, two degenerate modes are coupled by virtue of some perturbation elements such as slots [8, 10] and cutting angles [11] on the patch resonators to construct dual-mode band-pass filters. Actually, the feeding scheme has aroused a great impact on the performance of the dual-mode filter [8].

In the microwave fields, a variety of artificial electromagnetic structures have been recently presented and designed based on 2D or 3D periodic structures and have been applied to design of microwave devices with unique electromagnetic characteristics. Artificial electromagnetic structures have been reported, including Photonic Band-Gap (PBG), Electromagnetic Band-Gap (EBG), Defected Ground Structure (DGS), left-handed materials (Left-Handed Material, LHM), and Composite Right/Left-Handed (CRLH) [12]. These artificial electromagnetic structures have achieved good results in the application of the microwave field.

In 1999, Pendry et al. proposed a Split Ring Resonator (SRR) [13], which has since been used as an artificial electromagnetic structure in various microwave planar structures and circuits. After researchers, such as Pendry proposed the SRR of the split-ring resonator, Bonache et al. proposed the concept of a Complementary Split Ring Resonator (CSRR) [14], which is complementary to SRR and applied to microwave devices. Since the CSRR structure can produce a negative dielectric constant effect, it has been proven to play a huge role in reducing the size. In 2010, Q.-L. Zhang, et al. proposed a new type of evanescent-mode substrate integrated waveguide (SIW) band-pass filter with complementary SRRs [15], and both positive and negative couplings are obtained between the CSRRs by changing their locations and orientations. The proposed filters have a wide upper stopband.

In this paper, the CSRR structure is innovatively used as the perturbation element of the dual-mode patch filter. Instead of the ground plane, the etching process is made on the patch conductor to achieve the degenerate mode separation. At the same time, two out-of-band transmission zeros can occur as well, and the overall size of the dual-mode filter can be reduced to a certain degree. In order to further analyze the influence of this CSRR structure on the dual-mode patch filter, not only its parameters are discussed, but also similar structural analysis and comparisons are presented.

2. PROPOSED FILTER STRUCTURE

Figure 1 shows the structure of the proposed square patch band-pass filter. The gray region is a metal patch and a microstrip feed line, and the white region is a dielectric substrate under the metal, with

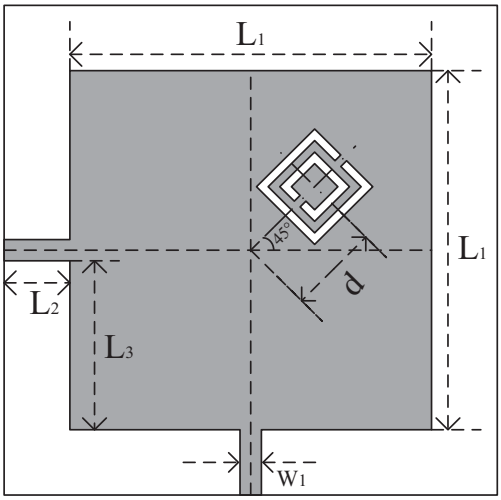

Figure 1. Geometry of the proposed square patch filter with a CSRR split.

a part of the metal patch hollowed out. The resonant cavity of the dual-mode filter adopts a square patch structure, and the perturbation element is a CSRR slit structure which is placed at a distance d from the center of the patch and at an angle of 45 degrees from the horizontal direction. For the feeding scheme of the filter, there are two types of direct feed and coupled feed. According to characteristics of the parallel coupling line, the coupling feeding method is better for the stopband, but a larger coupling gap will cause increased in-band insertion loss, and a smaller coupling gap will make the processing precision difficult to control. In order to reduce the insertion loss and improve the accuracy of the production, the filter adopts direct-connected feed-lines [8]. The input and output ports are in a 90 degree orthogonal relationship and are located at the midpoint of the two sides of the square patch. In order to ensure that the characteristic impedance of the two ports of the filter is $50\,\Omega$, the width $W1$ of the microstrip feeder is selected as 1.3 mm. The parameters of the patch band-pass filter structure are chosen as $d = 5$ mm, $L1 = 22$ mm, $L2 = 4$ mm, $L3 = 10.35$ mm.

In addition, it should be noted that the entire dielectric substrate has a size of $30 \times 30\,\text{mm}^2$ and a thickness of 0.508 mm, and the ground contact surface of the bottom surface has the same size as the dielectric plate. The selected dielectric substrate is Rogers 4003 with the dielectric constant 3.38. The geometry and dimension of the CSRR split are shown in Fig. 2. The specific parameters of the CSRR element are given: $L4 = L5 = 5$ mm, $L6 = L7 = 3$ mm, $G1 = G2 = G3 = 0.5$ mm, and $W2 = W3 = 0.5$ mm.

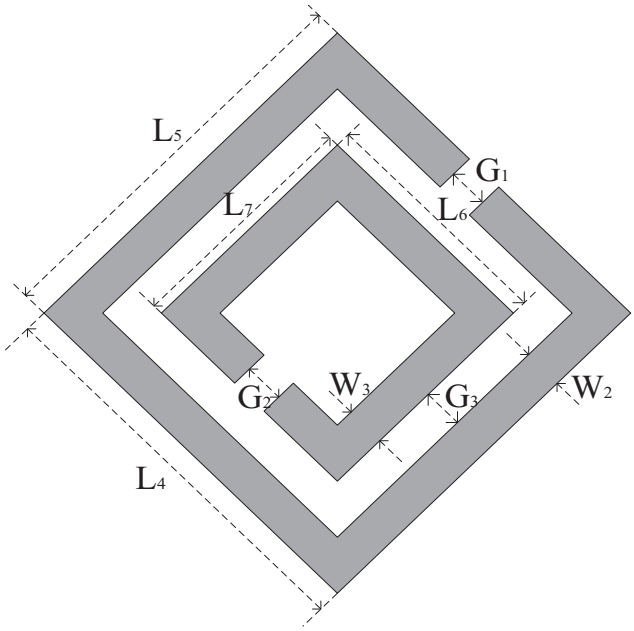

Figure 2. Structure of the proposed CSRR split.

3. PARAMETER ANALYSIS AND INVESTIGATION

As discussed above, by using the CSRR split as a perturbation element of the patch resonator, performance of the patch band-pass filter can get improved. In order to study the influence of the CSRR perturbation element on the performance of the dual-mode filter, the distance d between the center of this CSRR element and the square patch center is changed. A set of simulated results are obtained in the electromagnetic simulation software HFSS, as shown in Fig. 3.

As can be seen from Fig. 3(a), as the position of the CSRR perturbation element varies, the two degenerate resonant modes are both changed. The position of the CSRR perturbation element has a big effect on the return loss of the dual mode filter. In addition, as can be seen from Fig. 3(b), as the position of the CSRR element varies, the positions of the two transmission zeros are both changed as well, but the center frequency of the filter remains basically unchanged. At the same time, it can be

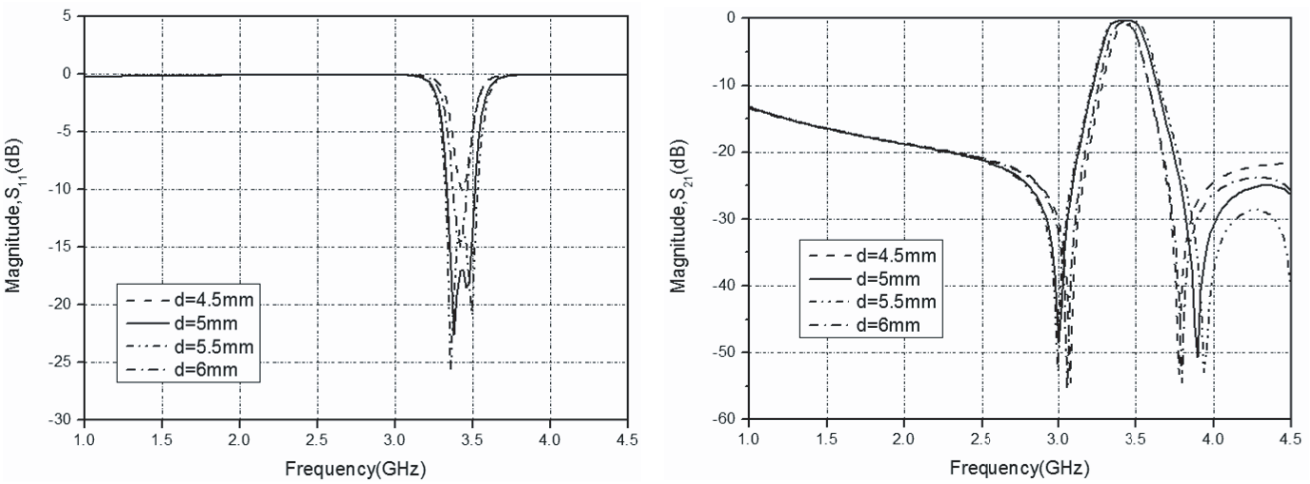

Figure 3. Geometry and Simulation results of the proposed square patch filter with CSRR split due to different locations of CSRR. (a) Magnitude of S_{11}; (b) Magnitude of S_{21}.

found through simulation that as the opening direction of the CSRR perturbation element is rotated by 180 degrees, that is, opposite to the opening direction in Fig. 2, the phenomenon of perturbation disappears, and the passband of the dual-mode filter disappears around 3.4 GHz.

According to the work in [16], the coupling coefficients between the two modes can be calculated by the following formula:

$$K = \frac{f_2^2 - f_1^2}{f_2^2 + f_1^2} \tag{1}$$

In these two degenerate modes, there are two higher and lower resonant frequencies, as denoted by f_1 and f_2 in Eq. (1). As shown in Fig. 4, the simulated two resonant frequencies and coupling coefficient versus the location parameter of CSRR are well known. With increasing the distance between CSRR split and the center of the substrate, the frequency of mode 1 tends to decrease, and that of mode 2 tends to increase. When d increases, the coupling coefficient K gradually increases.

In the HFSS simulation software, the electric field vector distribution of the two resonant modes is then simulated. By using the CSRR perturbation element, a set of degenerate modes of the same

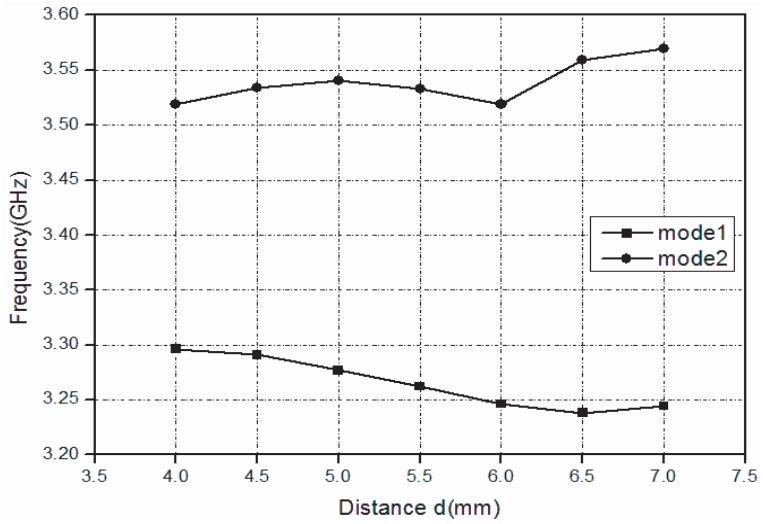

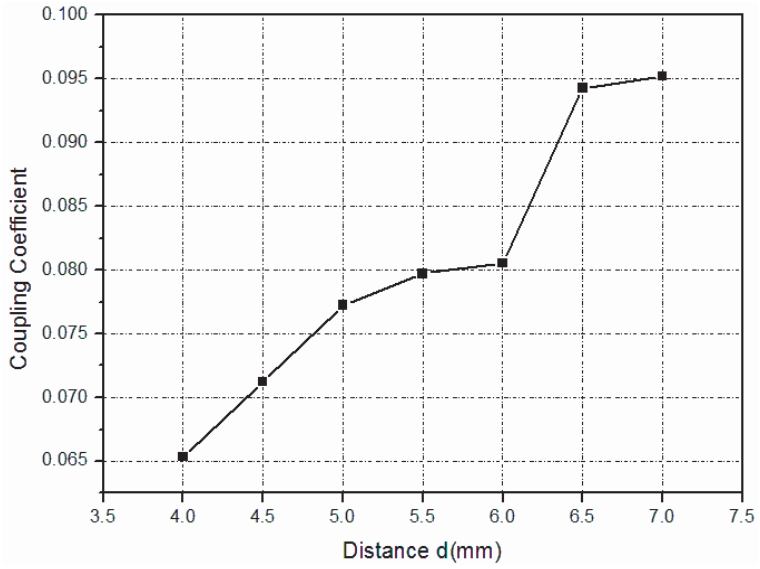

(b)

Figure 4. (a) Two resonant frequencies of the degenerate modes as a function of different distances d; (b) Corresponding coupling coefficients as a function of different distances d.

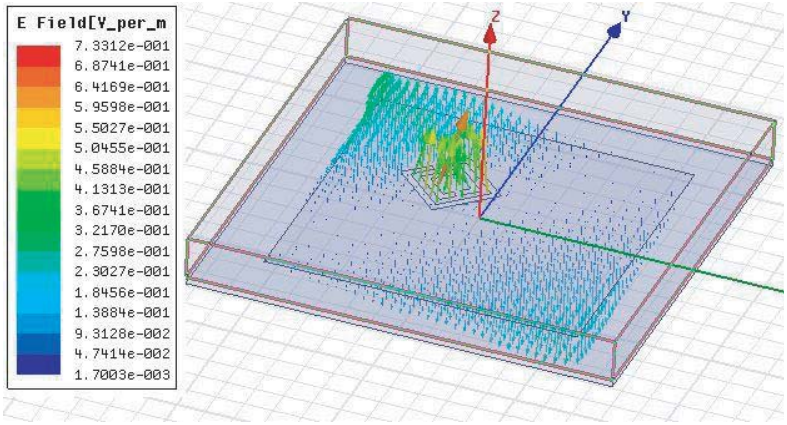

(a)

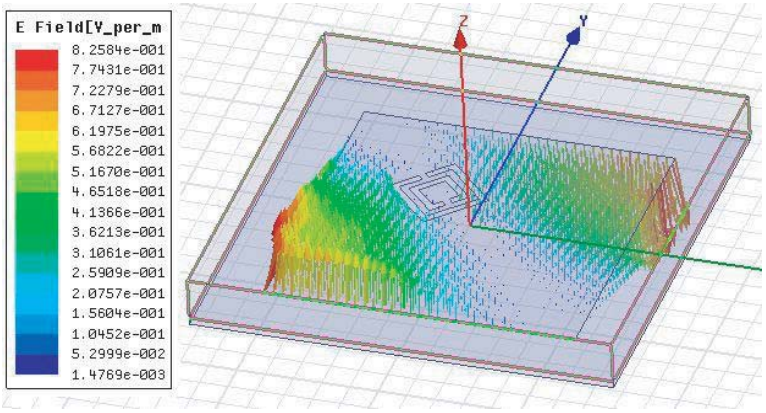

(b)

Figure 5. Electric field vector distribution of two resonant modes in HFSS. (a) Mode1; (b) Mode2.

frequency get separated, resulting in two different resonant frequencies. Figs. 5(a) and 5(b) show the electric field distributions of the first and second modes, respectively. The distinctive distributions of these two modes under the CSRR perturbation can be clearly seen from Fig. 5.

4. SIMULATION AND EXPERIMENTAL RESULTS

4.1. Simulation Results

In combination with the analysis and simulation of each size parameter of the filter, the optimal size of the square patch dual-mode filter is finally determined. Fig. 6 shows the simulated results for the patch dual mode filter. As can be seen from Fig. 6, the center frequency is about 3.42 GHz, the fractional bandwidth about 3.5%, the insertion loss of the filter in passband less than 1 dB, and the return loss of the filter in the frequency range from 3.36 to 3.48 GHz exceeds 15 dB. The filter has two out-of-band transmission zeros at 3.0 and 3.9 GHz with attenuations of 48 and 50 dB, respectively, and these two transmission zeros can be obtained without changing the feed and floor structure.

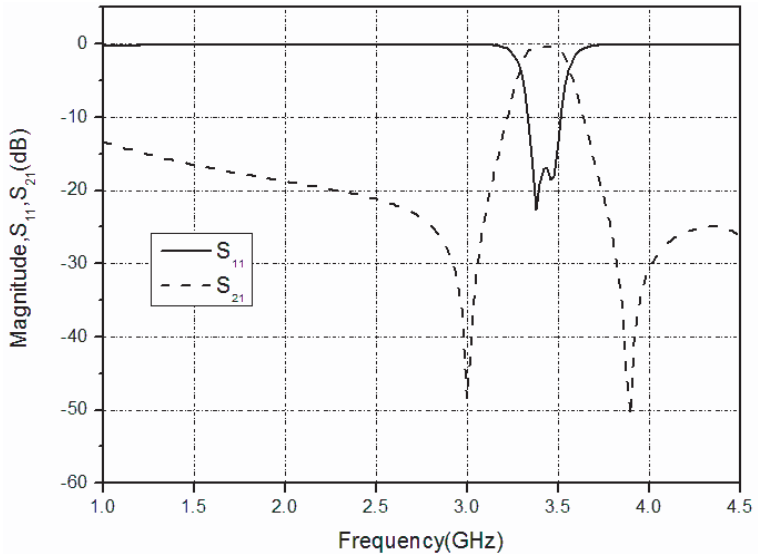

Figure 6. Simulation results of the proposed square patch filter.

4.2. Experimental Verification

In order to verify the accuracy of the simulation results, the dual-mode patch filter is then physically fabricated and measured. The size of the processed sample is consistent with the previous data. The dielectric constant, plate, and thickness of the dielectric substrate are the same as those in simulation. A photograph of the physical sample is shown in Fig. 7. The dual-mode filter is measured by a vector network analyzer. Fig. 8 shows the comparison of the simulated and measured results, which are found in good agreement with each other.

In Fig. 8, the solid line is the physical measured result, and the dotted line is the simulated result. It can be found herein that the measured center frequency slightly shifts to the low frequency compared with the simulated one. Due to the loss of metal caused by actual processing, the insertion loss increases, and impedance matching slightly deteriorates. From the measured results, the center frequency is about 3.3 GHz, the fractional bandwidth about 4.2%, and the return loss greater than 10 dB from 3.23 to 3.37 GHz. The insertion loss curve of the physical filter is basically the same as the simulation curve in shape. Two transmission zeros are still distributed on both sides of the passband, and the in-band insertion loss is less than 2.5 dB. The transmission zero attenuations at 2.925 and 3.825 GHz are equal to 40.4 and 43.6 dB, respectively.

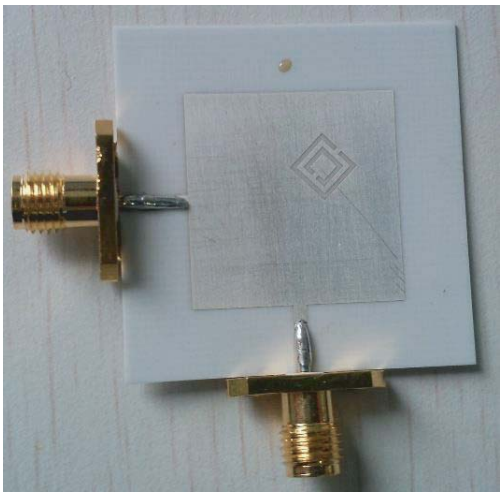

Figure 7. Photograph of the fabricated dual-mode band-pass filter.

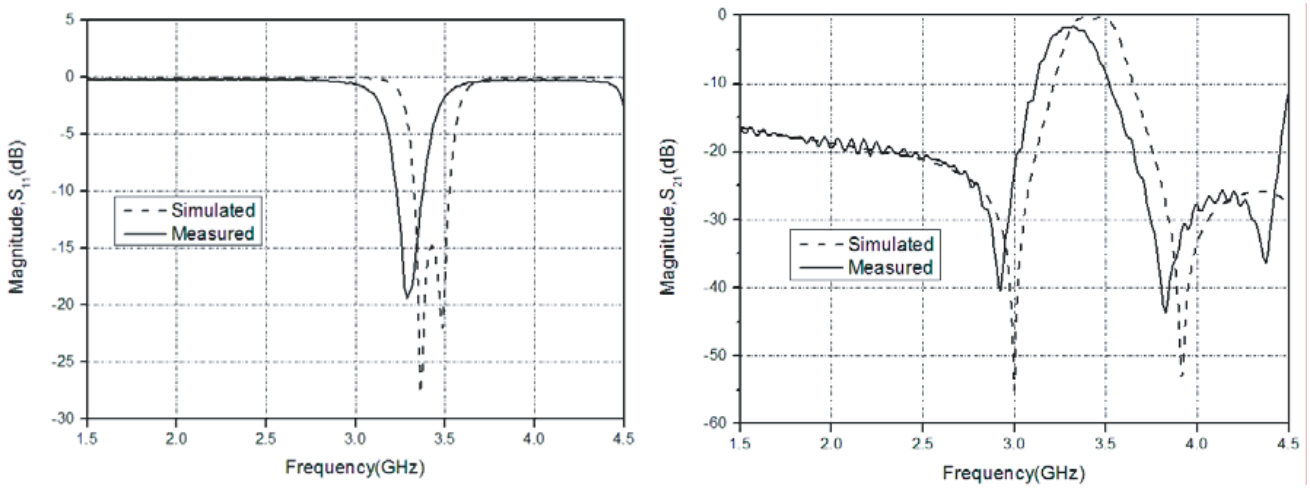

Figure 8. Simulation and measurement results of the proposed filter. (a) Magnitude of S_{11}; (b) Magnitude of S_{21}.

5. COMPARISON AND DISCUSSION

From the above discussion, it can be found that the position of the CSRR perturbation element and the direction of the opening have a great influence on the performance of the dual-mode filter. In order to investigate the characteristic of the dual-mode patch filter with CSRR perturbation further, a dual-mode filter with novel perturbation element is proposed for comparison. Since the intensity and nature of the coupling between the degenerate modes of the dual-mode resonator are determined by the size and shape of the perturbation element [7], the investigation on the perturbation element is particularly important. In this section, in order to further investigate the role of the CSRR perturbation element, the structure is changed in such a way that the CSRR inner small ring in Fig. 2 is removed to form a perturbation element with only one rectangular annular slot. Through simulation and fabrication, it can be found that the perturbation element of the single rectangular ring gap can also perturb the square patch cavity to form a dual-mode patch filter. The measured results have more obvious dual-mode characteristics. The structure of this dual-mode patch filter using single-loop perturbation is shown in Fig. 9.

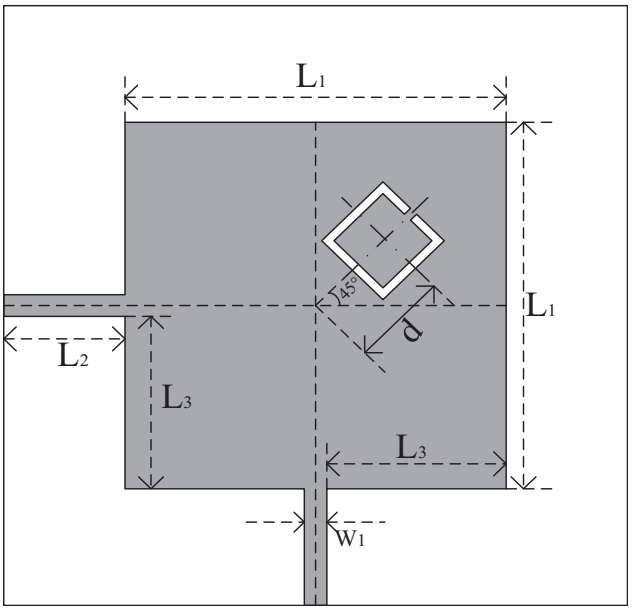

Figure 9. Geometry of the proposed square patch filter with a rectangular ring slot.

As can be seen from Fig. 9, both orthogonal feeding scheme of 90 degrees and the cavity are still used. The square patch cavity is different only by removing the inner small ring of the CSRR slot. Herein, the outer rectangular slot is used for the perturbation. In Fig. 9, the gray part is still the metal patch and microstrip feed line; the white part is the dielectric substrate under the metal; and the hollowed out part of the metal patch is a rectangular single ring gap. The center distance between the rectangular single-ring slit and the patch is d, which is 45 degrees from the horizontal direction. Thus, we can figure out that this filter structure is further simplified compared to the CSRR perturbation dual-mode filter before.

Under the selected substrate with relative dielectric constant of 3.38 and the thickness of 0.5 mm, the total area of the patch is equal to $22 \times 22\,\text{mm}^2$, and thus the filter is very compact. In order to

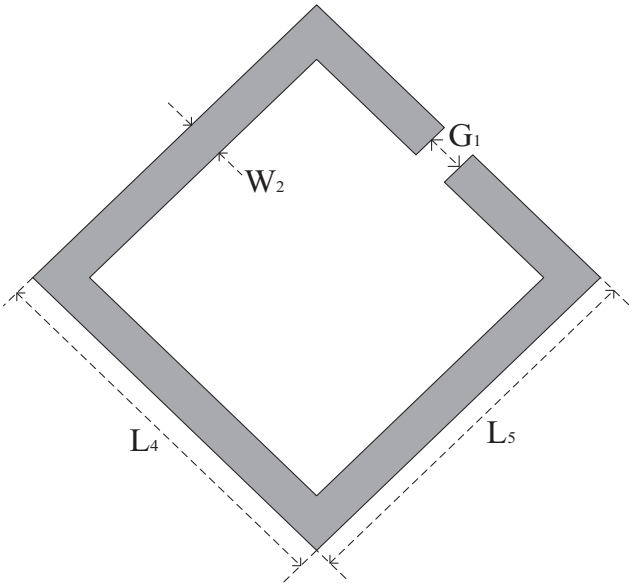

Figure 10. Structure of the proposed rectangular ring slot.

be convenient for connecting SMA joints and testing, the substrate area is reasonably expanded. In this way the total area of the substrate is $36 \times 36\,\text{mm}^2$, and the ground plane has the same size as the substrate. Two feed-lines are designed to satisfy the characteristic impedance of $50\,\Omega$, so the width of both lines is derived as $W1 = 1.1\,\text{mm}$. The parameters of the patch band-pass filter structure are chosen as $d = 5.5\,\text{mm}$, $L1 = 22\,\text{mm}$, $L2 = 7\,\text{mm}$, $L3 = 10.45\,\text{mm}$.

Meanwhile, the geometrical structure of the rectangular ring slot is shown in Fig. 10. The parameters of this novel perturbation element are given by: $L4 = L5 = 5\,\text{mm}$, $G1 = 0.5\,\text{mm}$, $W2 = 0.5\,\text{mm}$. It can be seen herein that the structure in geometry becomes much simpler than the first perturbation element, i.e., CSRR split.

In order to illustrate the influence of the single-loop perturbation structure on the performance of the dual-mode filter, the distance d between the center of the single-ring slot and the center of the square patch is further changed. A set of simulation results are obtained in the HFSS software, as shown

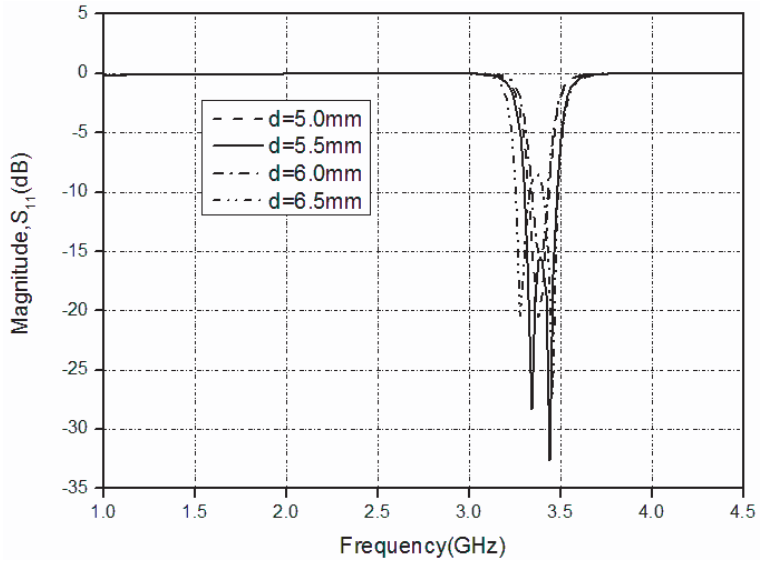

(a)

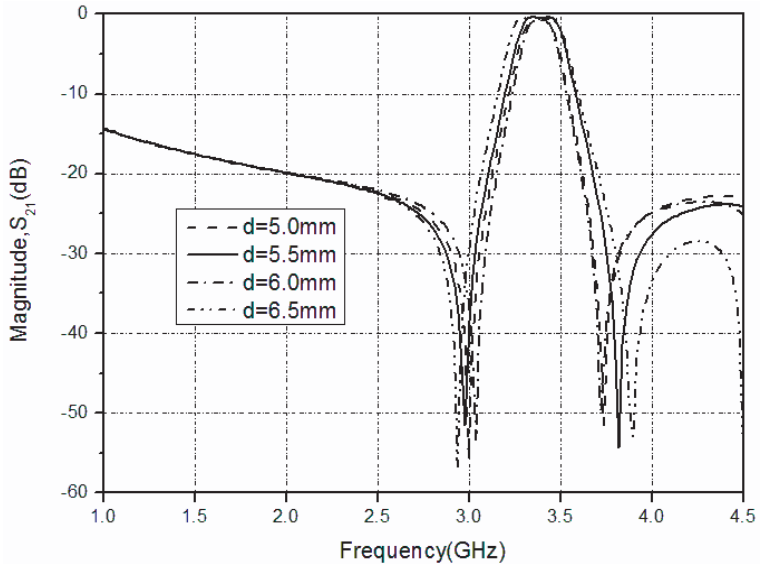

(b)

Figure 11. Simulation results due to different locations of the perturbation element. (a) Magnitude of S_{11}; (b) Magnitude of S_{21}.

in Fig. 11, indicating slight variation of its passband.

As can be seen from Fig. 11, the use of a rectangular single-ring slit as a perturbation element of a square patch resonator can also achieve the effect of separating the degenerate modes in the resonant cavity and produce dual-mode properties. From the simulation results, the dual-mode characteristic is even more obvious than the simulation results of CSRR perturbation at the optimal position where d is 5.5 mm. It can be seen that when CSRR is used as the perturbation element of the dual-mode patch resonator, the outer rectangular single-ring gap plays a major perturbation role.

By adjusting the position of the perturbation element, feed line width, patch size, and other structural parameters, the optimal size of the single-loop perturbation dual-mode filter is finally obtained. The simulation results of the dual-mode filter are shown in Fig. 12. Comparing Fig. 6 with Fig. 12, it can be seen that the single-loop perturbation dual-mode filter has more obvious dual-mode characteristic than CSRR perturbation dual-mode filter in the case of the same dielectric plate

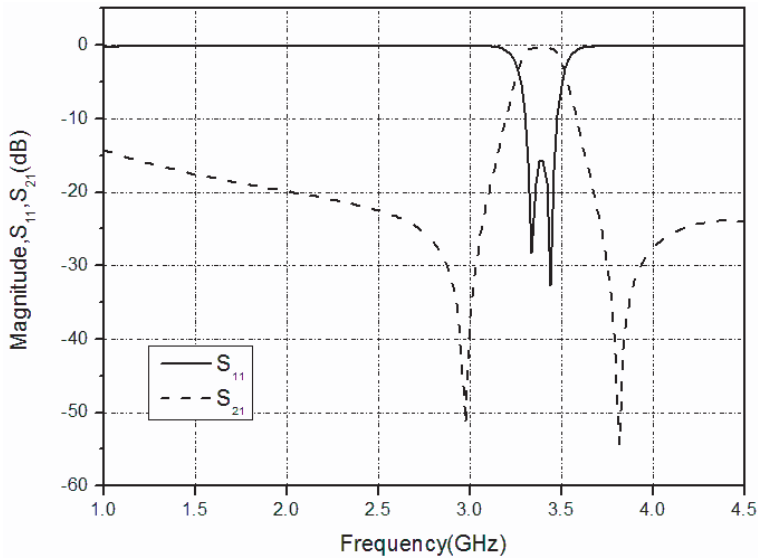

Figure 12. Simulation results of the square patch filter with a rectangular ring slot.

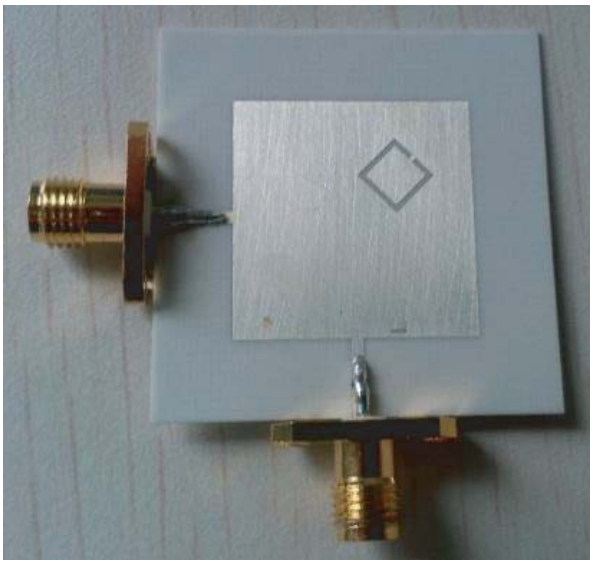

Figure 13. Photograph of the fabricated dual-mode band-pass filter with a rectangular ring slot.

and patch size, and the passband moves slightly to the low frequency. The effect is better than the dual-mode filter of the CSRR perturbation element. In the frequency range of 3.32 to 3.46 GHz, the center frequency is about 3.39 GHz and the fractional bandwidth about 4.1%, and the filter has a return loss greater than 15 dB and an insertion loss less than 1 dB. The filter has two out-of-band transmission zeros at 2.98 and 3.82 GHz with attenuations of 51 and 54 dB, respectively.

To verify the simulation results, the physical processing and measurement of the dual-mode filter using single-loop perturbation is further performed. The size of the processed sample is consistent with that in the previous section. The dielectric substrate is also Rogers 4003 with dielectric constant of 3.38 and thickness of 0.5 mm. A photograph of the physical sample is depicted in Fig. 13. Fig. 14 reveals that the measured results of the filter are in good agreement with the simulated ones in a wide frequency range.

Figure 14 shows the comparison between the simulated and measured results of the proposed dual-

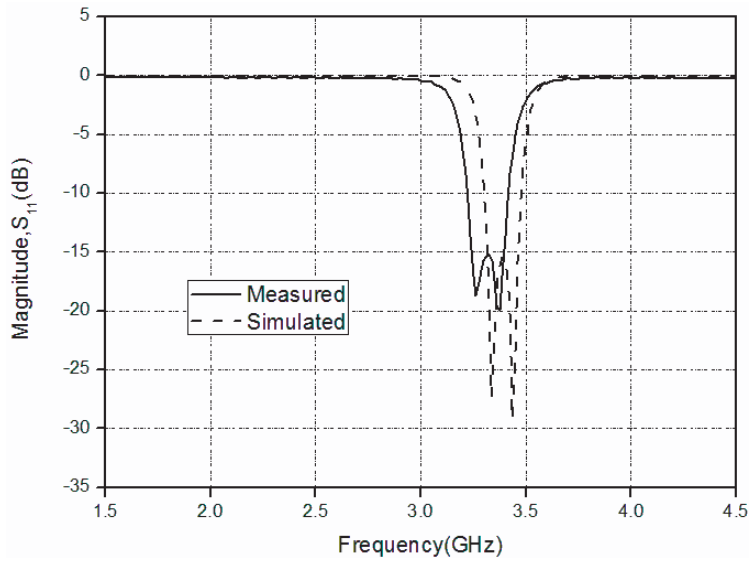

(a)

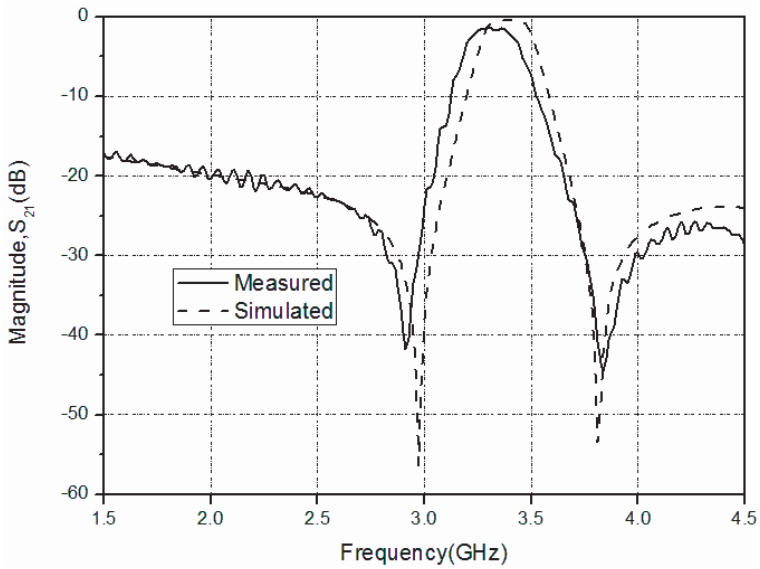

(b)

Figure 14. Simulation and measurement results of the second filter. (a) Magnitude of S_{11}; (b) Magnitude of S_{21}.

mode band-pass filter. It can be found herein that the measured frequency responses of this dual-mode band-pass filter with rectangular ring slot have exhibited very good dual-mode filtering performance. As seen from Fig. 14, the measured and simulated curves of the dual-mode filter are very similar to each other, and the measured curve is slightly shifted to the low frequency. The measured S_{11} has a good dual-mode behavior, which further proves that a single-loop structure can also perform the desired perturbation function to form a dual-mode filter with improved performance. From the measured data, the measured return loss of the single-loop perturbed dual-mode filter is greater than 10 dB from 3.23 to 3.41 GHz, the center frequency about 3.32 GHz, the fractional bandwidth about 5.4%, and the measured insertion loss less than 2 dB in the frequency range of 3.25 to 3.38 GHz. The sample filter indeed has a transmission zero attenuation of 41.7 dB at 2.91 GHz and a transmission zero attenuation of 44.6 dB at 3.84 GHz, as expected in design.

6. CONCLUSION

In this paper a dual-mode band-pass filter constituted by a square patch resonator is proposed and designed by using the CSRR split as a square patch resonator perturbation element. The dual-mode filter with CSRR structure perturbation has been analyzed, designed, and discussed in detail. The dual-mode filter with CSRR perturbation can produce two out-of-band transmission zeros, good passband matching, and small insertion loss. Through the processing measurement, it has been demonstrated that the measured results of the designed filter are basically consistent with the simulation ones; the performance is good; the volume is small; and the correctness of the design is verified. In order to analyze the CSRR split further, a dual-mode band-pass filter with a rectangular ring slot is then proposed to provide the comparative study on perturbation characteristics. It can be well understood that the dual-mode band-pass filter with the rectangular ring slot can achieve good dual-mode filtering characteristics.

ACKNOWLEDGMENT

This work was supported in part by the National Natural Science Foundation of China (Grant No. 61471204), the National and Local Joint Engineering Laboratory of RF Integration and Micro-Assembly Technology (Grant No. KFJJ20170206), Jiangsu Natural and Science Foundation of Universities (No. 13KJA510002) and Research Project of Nanjing University of Posts and Telecommunications (No. 208035).

REFERENCES

1. Wolff, I., "Microstrip bandpass filter using degenerate modes of a microstrip ring resonator," *Electron. Lett.*, Vol. 8, No. 12, 302–303, June 1972.
2. Chen, J. X., J. Li, and J. Shi, "Miniaturized dual-band differential filter using dual-mode dielectric resonator," *IEEE Microwave and Wireless Components Letters*, Vol. 28, No. 8, 657–659, Jun. 2018.
3. Gómez-García, R., J.-M. Muñoz-Ferreras, and W. J. Feng, "Balanced symmetrical quasi-reflectionless single-and dual-band band-pass planar filters," *IEEE Microwave and Wireless Components Letters*, Vol. 28, No. 9, 798–800, Aug. 2018.
4. Choudhury, S. R., A. Sengupta, and S. Das, "Band-pass filters using multilayered microstrip structures," *2018 Emerging Trends in Electronic Devices and Computational Techniques (EDCT)*, 8–9, Kolkata, 2018.
5. Hong, J. S. and M. J. Lancaster, "Microstrip band-pass filter using degenerate modes of a novel meander loop resonator," *IEEE Microwave and Guided Wave Letters*, Vol. 5, No. 11, 371–372, Nov. 1995.
6. Cheng, K.-K. M., "Design of dual-mode ring resonators with transmission zeros," *Electronics Letters*, Vol. 33, No. 16, 1392–1393, Jul. 1997.

7. Das, T. K. and S. Chatterjee, "Harmonic suppression in an in-line Chebyshev band-pass filter by asymmetrical perturbations," *2017 IEEE MTT-S International Microwave and RF Conference (IMaRC)*, 11–13, Ahmedabad, 2017.
8. Sung, Y., "Compact and low insertion loss dual-mode band-pass filter," *Microwave and Optical Technology Letters*, Vol. 50, No. 12, 3201–3206, Dec. 2008.
9. Zhang, R. Q., L. Zhu, and S. Luo, "Dual-mode dual-band bandpass filter using a single slotted circular patch resonator," *IEEE Microwave and Wireless Components Letters*, Vol. 22, No. 5, 233–235, Apr. 2012.
10. La, D. S., X. L. Ma, H. Y. Chen, and Y. P. Wu, "Novel dual-mode patch band-pass filters with slot structures," *Microwave and Optical Technology Letters*, Vol. 54, No. 9, 2130–2133, Sept. 2012.
11. Akgun, O., B. S. Teekici, and A. Gorur, "Reduced-size dual-mode slotted patch resonator for low-loss and narrowband band-pass filter applications," *Electronics Letters*, Vol. 40, No. 20, 1275–1277, Sept. 2004.
12. Huang, J. Q. and Q. X. Chu, "Compact UWB band-pass filter utilizing modified composite right/left-handed structure with cross coupling," *Progress In Electromagnetics Research*, Vol. 107, 179–186, 2010.
13. Pendry, J. B., J. Holden, D. J. Robbins, and W. J. Stewart, "Magnetism from conductors and enhanced nonlinear phenomena," *IEEE Transactions on Microwave Theory and Techniques*, Vol. 47, No. 11, 2075–2084, Dec. 1999.
14. Bonache, J., F. Martín, F. Falcone, and J. D. Baena, "Application of complementary split-ring resonators to the design of compact narrow band-pass structures in microstrip technology," *Microwave and Optical Technology Letters*, Vol. 46, No. 5, 508–512, Sept. 2005.
15. Zhang, Q. L., W. Y. Yin, and S. He, "Evanescent-mode Substrate Integrated Waveguide (SIW) filters implemented with complementary split ring resonators," *Progress In Electromagnetics Research*, Vol. 111, 419–432, 2011.
16. Hong, J. S. and M. J. Lancaster, *Microstrip Filters for RF/Microwave Applications*, 256–258, John Wiley & Sons, Inc., New York, 2001.